Research Article
Evaluation of Earthquake-Induced Risks in Modern, Code-Conforming Reinforced Concrete Moment Frames

Mehrdad Shokrabadi, Mehdi Banazadeh and Mehran Shokrabadi
Department of Civil and Environmental Engineering, Amirkabir University of Technology, Tehran, Iran

Abstract: The main objective of this study is to employ performance assessment procedure to evaluate earthquake-induced risks in modern, code-conforming Reinforced Concrete (RC) moment frames in terms of collapse risk and possible financial losses. In order to accomplish this goal, a set of 15 archetype RC moment frames is evaluated in this study. The buildings are different regarding height and structural system ductility. The archetypes are assumed to be located in three zones with different levels of seismicity. The findings of the collapse assessment procedure indicate that the constraint of ASCE 7-05 for the lower limit of design base shear has the most significant impact and the ductility has the least influence on collapse risk. Also, it has been found that buildings located in the low seismicity zone have significantly lower levels of losses. Sensitivity analysis is employed to study the variations of earthquake consequences due to the variations in the design decisions.

Keywords: Collapse risk, human and monetary consequences of earthquake, performance-based earthquake engineering

INTRODUCTION

The reliance of current seismic design provisions on the empirical and judgmental axis will put a question on the ability of these codes in providing approximately uniform risk against earthquake among all the conforming buildings. This study applies the Performance-Based Earthquake Engineering (PBEE) methodology through the nonlinear dynamic time history analysis to assess the seismic performance of a set of 15 reinforced concrete moment framearche types. The set of archetypes are designed to be in accordance with the requirements of ASCE 7-05 (ASCE, 2005) and ACI 318-05, (2005). In this study, taking advantage of the collapse assessment methodology proposed by Haselton and Gregory, (2007) and Liel and Deierlein (2008) and the FEMA P-58 (FEMA, 2012) recommended loss evaluation process, we focus on expanding the previous findings to the buildings located in different seismic zones and having distinct levels of structural ductility to examine to which extent the modern loading and design provisions are successful in achieving an approximately uniform seismic risk.

With the purpose of clarifying how the variations in height, ductility and seismicity would affect the seismic risk in modern code-conforming RC moment frames, the set of representative archetypes is selected to include 4-, 8- and 12-story buildings with the lateral-resisting structural system consists of ordinary, intermediate and special perimeter moment frames. The buildings are sited in regions with three different levels of seismic hazard including low, moderate and high seismicity. The differences between the outcomes of the collapse assessment and loss prediction processes among the set of the set of archetypes are investigated through the use of sensitivity analysis.

MATERIALS AND METHODS

Site selection and seismic hazard: The selected archetypes are located in Los Angeles, Las Vegas and Austin at which the ASCE-recommended Maximum Considered Earth quake (MCE) level 1-second spectral acceleration corresponds to the values of 0.912, 0.363 and 0.078 g, respectively. Site-specific seismic hazard parameters are extracted from the USGS hazard maps (USGS, 2012) for ASCE 7-05. Figure 1 compares the uniform hazard MCE spectra of ASCE 7-05 for the mentioned sites.

In order to perform Incremental Dynamic Analysis (IDA) (Vamvatsikos and Cornell, 2002), 22 pairs of far field ground motion records, which has been recommended by FEMA P-695 (FEMA and ATC, 2009), is employed. The intensity measure for representing the intensity parameter and scaling the ground motions is selected to be the spectral acceleration at the first mode period with 5% coefficient of damping. In order to account for the important effect of spectral shape on the collapse
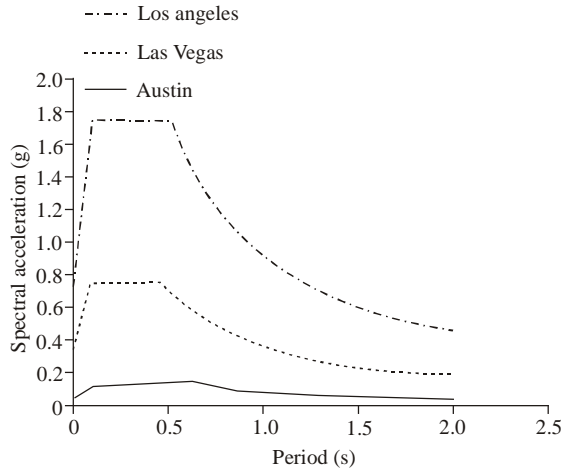
Fig. 1: Uniform hazard seismic design spectra for the selected sites

assessment results, outcomes of the collapse assessment procedure are modified using the method suggested by Haselton and Gregory (2007).

Archetypes design and specifications: In order to provide a robust base to investigate the differences that variations in design parameters of code-conforming RC buildings might induce in seismic risk, the set of archetypes is selected to represent the important parameters that variation among them is permitted in codified seismic provisions and these variations might impact the seismic performance of conforming structures. These variations include key design parameters such as height which is chosen to vary from 4 to 12 stories, ductility of the structural system which reflects in the three types of moment frames including special, intermediate and ordinary frames and finally the seismicity of the site in which the archetype are located and is represented by the three sites described in materials and methods section. The governing design criteria lies between the ASCE 7-05 loading provisions and ACI 318-05 design necessities for special, intermediate and ordinary RC frames. The lateral-force resisting structural system has the bay span of 6-m width. Story heights are 4 m in the first story and 3.3 m in all other above stories.

Structural nonlinear modeling and analysis: All of the archetypes are modeled through a two-dimensional model of the lateral-force resisting system using the OpenSEES (2012) platform. The gravity frames are not included directly in the models. However, the adverse $P - \Delta$ effects resulting from the additional tributary mass on the gravity frames are involved by applying these additional gravity loads on a leaning column.

Nonlinear modeling in this study has two different aspects. A fiber-type model is used for modeling beams and columns in lower levels of intensity at which

cracking and tension-stiffening effects are important and the fiber model is known to be more accurate than the plastic hinge model in capturing these effects. Beside the fiber model, because of the ability of the plastic hinge models in incorporating deterioration resulted from rebar buckling and concrete crushing, a lumped plasticity model is employed to simulate the nonlinear behavior of structures at high levels of intensity which finally leads to the collapse of structure. Collapse in this study is defined as the point of dynamic instability at which a minor increase in intensity will result in an infinite increase in response, which is defined here as the maximum of Interstory Drift Ratio (IDR). The nonlinear plastic hinge model for beams and columns employs a trilinear backbone curve and hysteretic rules introduced by Ibara *et al*. (2005) to simulate the nonlinear and hysteretic behaviors of the structural elements. The design and modeling uncertainties are incorporated by modifying the total dispersion of collapse fragilities regarding the method proposed by Haselton and Gregory (2007) and an assumed value of 0.45 for these types of variation. Haselton and Gregory (2007) showed that design and modeling uncertainties have a significant effect on the collapse assessment outcomes.

RESULTS AND DISCUSSION

Collapse assessment findings: The results of collapse assessment can be summarized in 4 major measures including one ductility-related measure namely maximum Interstory Drift Ratio (IDR_{col}) at collapse and three performance-related measures recognized as the collapse margin ratio defined as the ratio of the median of collapse spectral acceleration to the spectral acceleration with 2% probability of exceedance in 50 years, the probability of collapse conditioned on occurring the 2% in 50-year ground motion $\left(P\left[C\middle|Sa_{2/50}\right]\right)$ obtained from the collapse fragility curve and the mean annual frequency of collapse $\left(\lambda_{collapse}\right)$ which is the result of integration of collapse fragility function together with the site-specific hazard curve. Sensitivity analysis shows that variations in the design parameters causes the collapse margin ratio to range from 1.14 to 3.21, the probability of collapse to vary between 2 and 41% and the mean annual frequency of collapse to lie across 1.9×10^{-4} and 20×10^{-4}.

Trends between height and collapse performance: Figure 2 shows how the collapse margin ratio, for the whole set of frames, changes as the building height changes. The margin against collapse has a completely different trend for buildings located in the high and moderate seismicity regions (Los Angeles and Las
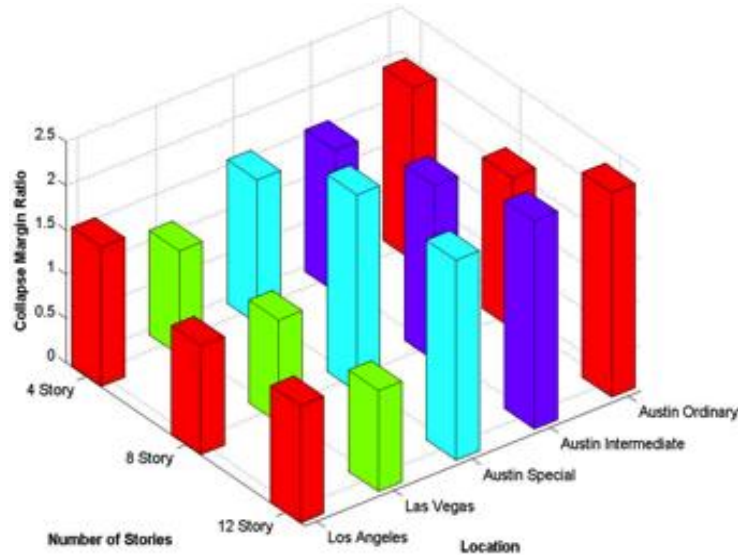
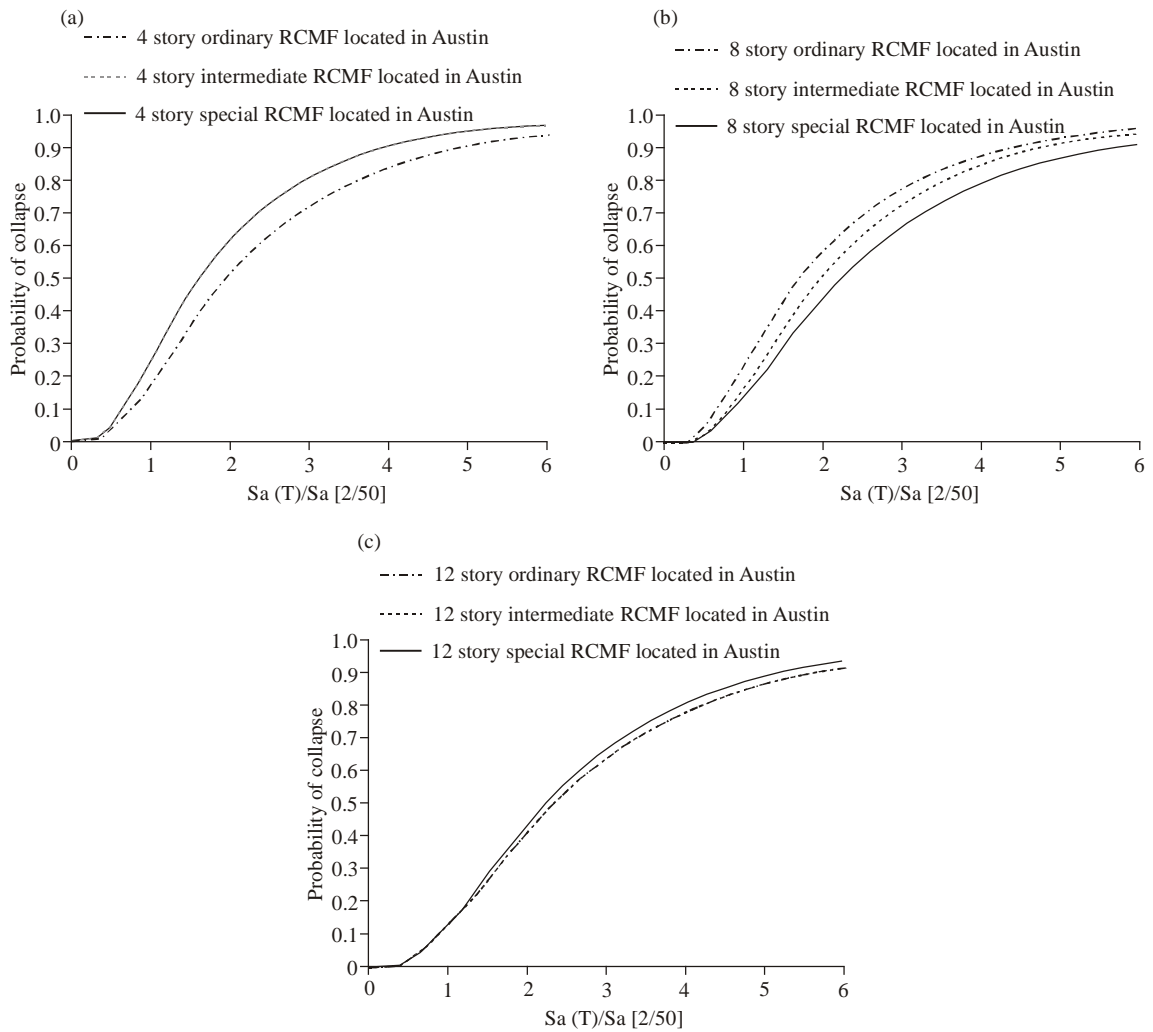Fig. 2: Collapse margin ratio for the whole set of frames

Fig. 3: Normalized collapse fragility curves for the special, intermediate and ordinary (a) 4-story frames, (b) 8-story frames and (c) 12-story frames located in Austin

Vegas) in comparison with the buildings located in the low seismicity region (Austin). For the buildings located in the sites with high and moderate seismic hazard, the collapse margin decreases as the building height increases. This reduction in collapse safety is primarily the result of the more significant $P - \Delta$ effects in the taller frames.

Although a similar trend is expected for the frames located in Austin, the constraint imposed by ASCE 7-05 for the lower limit of the design base shear coefficient (equation 12.8-5) makes the design base shear for the 8- and 12-story frames much more conservative and leads to the substantial improvement in the collapse performance of the taller buildings in Austin. The conservatism imposed by the equation 12.8-5 of ASCE 7-05 increases as the height of the buildings increases and thus leads to the better collapse performance for the taller buildings in Austin.

Trends between ductility and collapse performance:
Figure 3 compares the collapse fragility curves for the 4, 8- and 12-story special, intermediate and ordinary frames located in Austin. The horizontal axis is normalized by the 2% in 50-year ground motion. As illustrated in Fig. 3, the collapse fragility curves for all types of frames with the same height are approximately equal. One notable observation is the better collapse performance of the 4-story ordinary frame in comparison with the special and intermediate 4-story frames. This better collapse performance of the 4-story ordinary frame is the result of the higher design base shear coefficient of this frame and the low seismic hazard of Austin. The low seismic demands in Austin lead to the structural members (beams, columns) of considerably low stiffness which, despite the higher element-level ductility in special and intermediate frames, results in the intensified $P - \Delta$ effects in the columns and decreases the system-level ductility of all 3 types of frames. Additionally, the low seismic forces in the 4-story frames located in Austin considerably reduces the effects of the ACI 318 special seismic provisions such as the strong-column weak-beam ratio and the joint shear panel requirements and, as a result, virtually there would be no differences between the design outcomes of the 4-story special, intermediate and ordinary frames in Austin. As the height of the frames increases, these special seismic provisions become more effective and consequently the performance of the special and intermediate frames improves.

Trends between earthquake hazard and collapse performance: Figure 4 shows how median of the IDR at collapse, for the special frames located in the three considered zones, changes as the height increases. As the seismic hazard decreases, the reduction in the
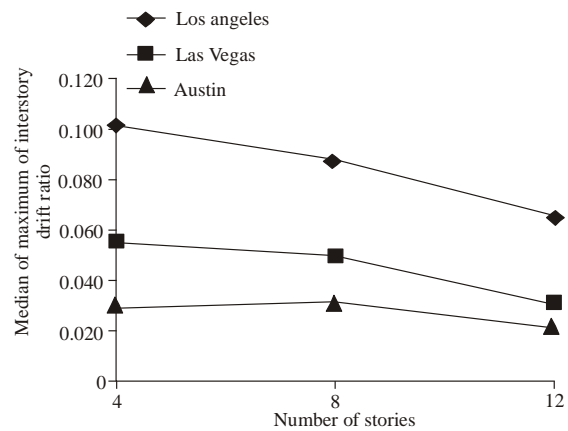

Fig. 4: Trends between the height and median of IDR at collapse for all of the special frames

stiffness of the structural members of frames leads to the intensified destabilizing $P - \Delta$ effects for the frames located in Austin and, as a result, the IDR at collapse decreases as the seismic hazard reduces. This reduction in the ductility might result in the misleading conclusion that the collapse performance of frames declines as the seismic hazard decreases. Figure 5, which compares the collapse fragility curves of 4-, 8- and 12-story special frames, shows that this conclusion is not generally true. The better collapse performance of the 8- and 12-story special frames located in Austin, as it is discussed in section 6.1, is the result of the constraint imposed by the equation 12.8-5 of ASCE 7-05. Specifically, the approximately negligible additional conservatism imposed by this equation on the 4-story frame located in Austin has caused this frame to have a collapse fragility curve nearly identical to that of the 4-story frame located in Los Angeles. However, the significant conservatism levels for the 8- and 12-story frames in Austin, which is the result of the restriction imposed by equation 12.8-5, has resulted in the better collapse performance in comparison with the similar frames located in the two other cities. The similarity between the collapse fragility curves of the frames located in Los Angeles and Las Vegas, despite the substantial differences in the return periods of design spectral accelerations, shows that this type of variation has virtually no impact on the collapse risk of the frames located in zones with different seismic hazard. However, this conclusion is based on a limited set of representative archetypes and, in order to generalize these conclusions, a large set of archetypes located in different seismic zones must be examined.

Financial consequences of earthquake: In this section, we further examine the seismic-induced risks by employing metrics for assessing the financial losses. As it has been emphasized by Liel and Deierlein (2008), the collapse performance is not solely a
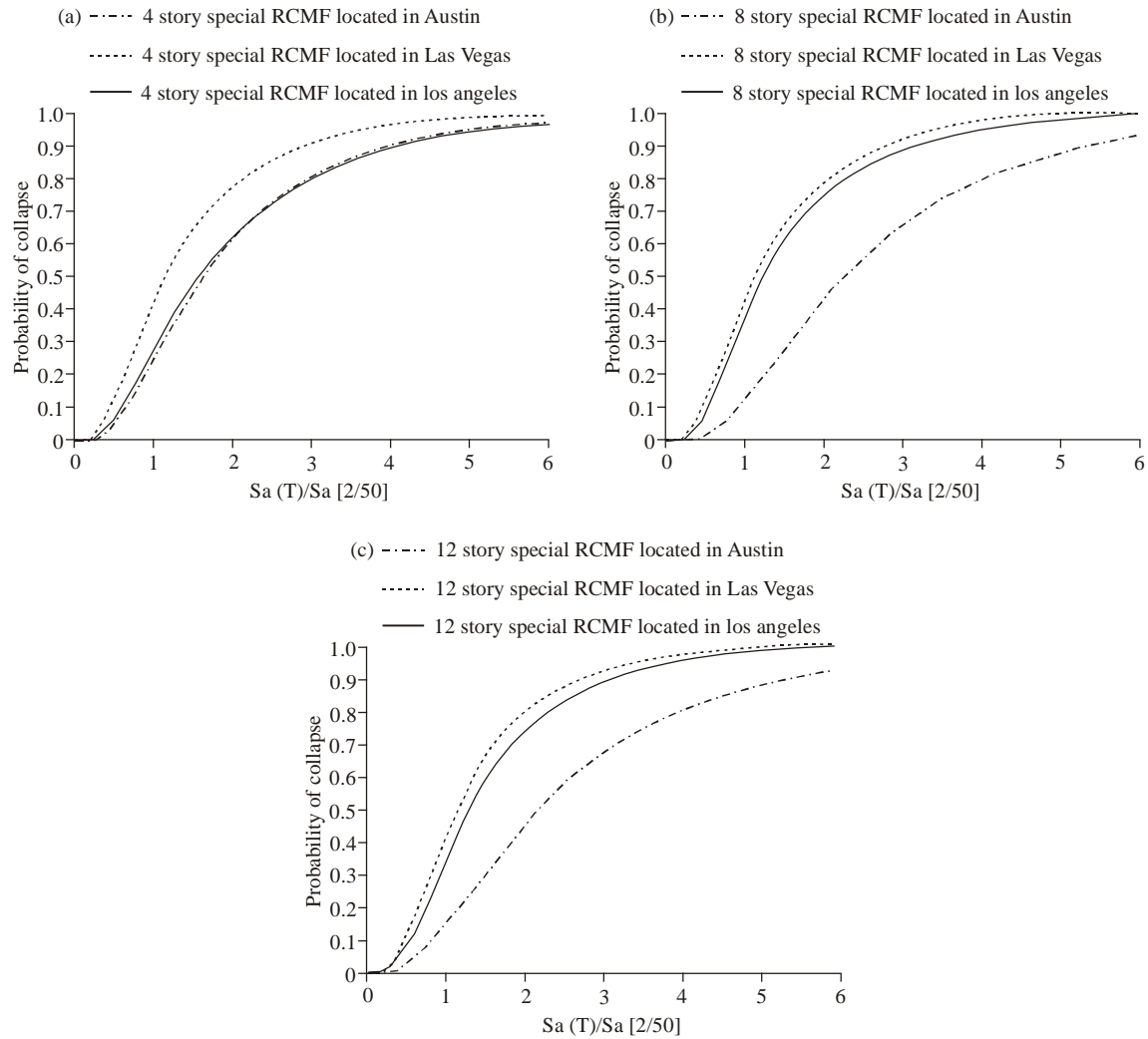
Fig. 5: Normalized collapse fragility curves for the special (a) 4-story frames, (b) 8-story frames and (c) 12-story frames located in Los Angeles, Las Vegas and Austin

Table 1: Loss assessment assumptions and findings

Design and framing			Initial assumptions			Loss assessment results		
Location	Stories	Type of the frame	Replacement cost (million dollars)	Replacement time (days)	Max number of occupants	Expected annual fatalities normalized by total occupants (%)	Expected annual repair cost normalized by replacement cost (%)	Expected annual repair time (days)
Los Angeles	4	Special	4.280	1140	58.00	0.003	1.46	12.07
	8	Special	10.510	1140	115.30	0.006	1.11	11.22
	12	Special	14.530	1140	173.00	0.005	0.88	9.95
Las Vegas	4	Special	4.180	1140	58.00	0.002	0.20	1.78
	8	Special	9.900	1140	115.30	0.005	0.28	3.05
	12	Special	14.150	1140	173.00	0.009	0.39	4.38
Austin	4	Special	3.060	1140	58.00	0.001	0.04	0.40
	8	Special	7.410	1140	115.30	0.001	0.03	0.29
	12	Special	10.540	1140	173.00	0.001	0.02	0.28
	4	Intermediate	3.060	1140	58.00	0.001	0.03	0.27
	8	Intermediate	7.410	1140	115.30	0.001	0.02	0.26
	12	Intermediate	10.540	1140	173.00	0.001	0.02	0.23
	4	Ordinary	3.060	1140	58.00	0.001	0.03	0.24
	8	Ordinary	7.410	1140	115.30	0.002	0.03	0.33
	12	Ordinary	10.540	1140	173.00	0.002	0.03	0.32

comprehensive measure for comparing seismic performance in structures with different configurations. Considering this issue, we have employed the approach proposed by FEMA P-58(FEMA, 2012) and its companion software, PACT 2(ATC, 2012), to evaluate the cost and time that shall be allocated for the repair of

seismic-induced damages. This method relies on the fragility curves to define the earthquake-induced damages to structural and non-structural components. The fragility curves used in this study are the lognormal probability distribution functions that, having the drift or acceleration induced in each story by the earthquake, give the probability of exceeding a particular damage state in each component. These metrics are measured using the expected annual criterion, obtained by integrating the diagram of cost versus intensity together with the site-specific hazard curve and is interpreted as the loss that occurs on average every year.

Before conducting the damage analysis for each building, some necessary assumptions must be made about the replacement cost and time of each building. To evaluate the replacement cost of each archetype, we referred to the RS Means (2012) assessments. The required time to replace a damaged structure is estimated using Mitrani-Reiser (2007) evaluations. All of these assumptions are brought in Table 1 for the whole set of archetypes. Table 1 also indicates the loss assessment results for all of the archetypes evaluated in this study. In order to make comparison possible among the different design alternatives, the results presented in the seventh and eighth columns of Table 1 are normalized with respect to the related presumptions summarized in the fourth and fifth columns of Table 1. As summarized in Table 1, the monetary losses are assessed using the expected annual losses as the evaluation parameter. Outcomes of Table 1 for the expected annual losses are plotted in Fig. 6. Results of the expected annual losses mainly depend on the

spectral accelerations with relatively low return periods. The earthquake-induced monetary losses at these levels of spectral acceleration are usually due to the damages to the interior partitions and structural elements (beams and columns). Therefore, it can be concluded that damages to these two types of components are mostly responsible for the expected annual financial losses. The damage states for both the interior partitions and beams and columns are the functions of IDR. As it is indicated in the fourth and fifth columns of Table 2, which present the mean and annual frequency of exceedance of the IDRs correspond to the most damaging spectral acceleration obtained from the 22 pairs of records for each archetype, the IDRs for buildings located in 3 different seismic zones are significantly different. The IDRs associated with the buildings located in Austin are substantially lower than those associated with the buildings located in Las Vegas and also IDRs for the buildings located in Las Vegas are considerably lower than those for the buildings located in Los Angeles. As summarized in Table 3, the mean of the IDRs that can lead to the first damage state in interior partitions and beams and columns are 0.002 and 0.02 respectively. Comparing these minimum damaging IDRs with the most damaging IDRs listed in Table 2, it can be observed that the IDRs in the zones with high seismic hazard is associated with the more severe damage states and more considerable monetary losses. Furthermore, the decrease of the IDR values with the reduction in the seismic hazard, which is mainly the result of the higher $P - \Delta$ effect, shifts the damaging intensities to the
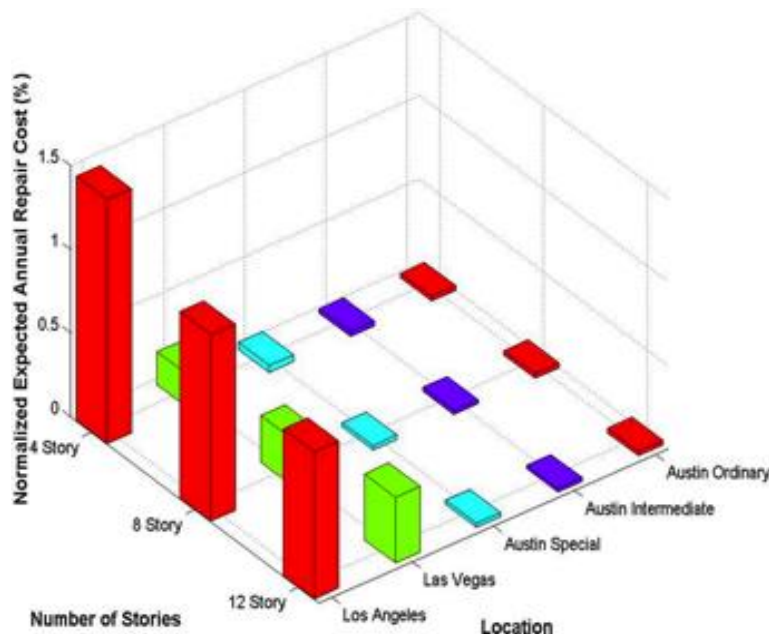

Fig. 6: Expected annual repair cost normalized by the replacement cost for the archetypes

Table 2: Most damaging spectral acceleration and collapse mechanism for the buildings

Archetype properties			Most damaging spectral acceleration		Collapse mechanism	
Location	Stories	Type of the frame	Annual frequency of exceedance	Mean of IDR	Number of stories engaged in collapse mechanism	Ratio of stories engaged in collapse mechanism to total number of stories
Los Angeles	4	Special	1.7E-02	0.0136	1.6	0.39
	8	Special	7.2E-03	0.0254	2.1	0.27
	12	Special	6.8E-03	0.0203	1.9	0.16
Las Vegas	4	Special	1.9E-03	0.0189	1.9	0.47
	8	Special	6.6E-03	0.0170	2.0	0.25
	12	Special	7.8E-03	0.0133	1.9	0.16
Austin	4	Special	1.2E-03	0.0067	1.7	0.43
	8	Special	5.6E-04	0.0074	2.9	0.36
	12	Special	4.8E-04	0.0113	1.9	0.16
	4	Intermediate	1.3E-03	0.0046	1.9	0.48
	8	Intermediate	5.9E-04	0.0084	2.6	0.33
	12	Intermediate	4.6E-04	0.0114	1.9	0.16
	4	Ordinary	1.3E-03	0.0058	2.1	0.50
	8	Ordinary	5.6E-04	0.0083	3.0	0.38
	12	Ordinary	3.9E-04	0.0125	1.4	0.12

Table 3: Fragility functions for beams and columns and interior partitions

Component	Damage states	Mean of damaging IDR (%)	Mean of repair cost (U.S. dollars)
Special frame	Concrete cracking	2.00	17200
	Cover concrete spalling	2.75	27700
	Concrete crushing and bars buckling	5.00	34000
Intermediate frame	Concrete cracking	2.00	17200
	Cover concrete spalling	2.50	27700
	Concrete crushing and bars buckling	3.50	34000
Ordinary frame	Concrete cracking	1.75	17200
	Cover concrete spalling	2.25	27700
	Concrete crushing and bars buckling	3.25	34000
Interior partitions	Light cracking	0.20	5300
	Moderate cracking	0.70	17000
	Significant cracking and crushing of gypsum wall boards	1.20	26400

ground motions with lower probability of occurrence in the zones with low seismic hazard, as indicated in Table 3. Considering the direct relation between the expected annual loss and hazard curve, the lower probability of occurrence for the damaging ground motions in Austin and Las Vegas leads to the significantly lower expected annual losses in these cities than the expected annual losses for the buildings located in Los Angeles.

CONCLUSION

In this study, we employed the performance-based earthquake engineering framework to evaluate the seismic-induced risks in modern, code-conforming RC moment frames which their design procedure stands among the constraints of ASCE 7-05 and ACI 318-05. The set of representative archetypes are selected so that the effects of variations in height, ductility and seismicity on the seismic risks can be examined. The assessment procedure is divided into two sections; in the first section the collapse performance of the archetypes and effects of the variations in the design parameters on collapse assessment outcomes is studied and in the second section monetary consequences of earthquake is compared for the set of structures.

Findings of the collapse assessment show that the margin against collapse lies between 1.2 and 2.4 with an average of 1.7 and the mean annual frequency of collapse varies from 3.5×10^{-4} to 20×10^{-4} with the mean value of 7.3×10^{-4}. Among the investigated design parameters, the collapse risk is mostly influenced by the minimum design base shear constraint of ASCE 7-05. Applying this constraint leads to the better collapse performance of the 8- and 12-story buildings in Austin than the 4-story frame because of the more conservative design base shear of the 8- and 12-sroty frames. For the frames located in Los Angeles and Las Vegas, in which the equation 12.8-5 of ASCE 7-05 does not affect the design base shear, collapse risk is relatively consistent over height with the taller frames being slightly more vulnerable to collapse because of the intensified $P - \Delta$ effects in the taller frames.

Comparing the collapse risk for the ordinary, intermediate and special frames, we found that the collapse risk does not significantly changes as the ductility of frames changes. Also, outcomes of the collapse assessment procedure shows that frames located in zones with different levels of seismic hazard have relatively similar collapse risks unless the constraint of the equation 12.8-5 of ASCE 7-05 makes the design base shear for 8- and 12-story frames located

in the zone with low seismic hazard significantly conservative and thus, enhances the collapse performance of these frames.

By conducting damage assessment procedure for the whole set of archetypes, this study shows that, expected annual losses due to earthquake occurrence varies significantly with the seismic hazard and buildings located in the zone with low seismic hazard have considerably lower losses.

Outcomes of the collapse assessment procedure of this study shows to which extent are the modern seismic requirements successful in providing uniform safety among the conforming structures with different configurations. Furthermore, findings of the loss assessment procedure can provide authorities, stakeholders and insurance companies with metrics to assess the financial risks associated with earthquake and contribute them in making decisions that lead to the minimization of adverse consequences of earthquake.

REFERENCES

ACI 318M-05, 2005. Building Code Requirements for Structural Concrete and Commentary. American Concrete Institue, ISBN: 9780870317446.

ASCE, ASCE/SEI 7-05., 2005. Minimum Design Loads for Buildings and Other Structures. American Society of Civil Engineers, Retrieved form: www.asce.org/Product.aspx?id=2147487569

ATC, 2012. Performance Assessment Calculation Tool (PACT) 2. Applied Technology Council (ATC).

FEMA, FEMA P-58, 2012. Seismic Performance Assessment of Buildings Volume 1 - Methodology. Applied Technology Council (ATC): Prepared for Federal Emergency Management Agency (FEMA); Retrieved form: https:// www. atcouncil. org/pdfs/ ATC- 58- 1/ FEMA P-58_ Volume1_Pre-Release August 2012. Pdf.

FEMA (Federal Emergency Management Agency) and ATC (Applied Technology Council), 2009. Quantification of Building Seismic Performance Factors. U.S. Dept. of Homeland Security, Washington, D.C.

Haselton, C.B. and G.D. Gregory, 2007. Gregory assessing seismic collapse safety of modern reinforced concrete moment frame buildings. Ph.D. Thesis, Stanford University.

Ibara, L.F., R.A. Medina and H.Krawinkler, 2005. Hysteretic models that incorporate strength and stiffness deterioration. Earthq Eng. Struct. Dyn., 34(12): 1489-1511.

Liel, A.B. and G.G. Deierlein, 2008. Assessing the collapse risk of california's existing reinforced concrete frame structures: Metrics for seismic safety decisions. Ph.D. Thieses, Stanford University.

Mitrani-Reiser, J., 2007. An ounce of prevention: Probabilistic loss estimation for performance-based earthquake engineering. Ph.D. Thesis, California Intitue of Technology.

OpenSEES, 2012. Open System for Earthquake Engineering Simulation (OpenSEES). Pacific Earthquake Engineering Research Center, 2.3.2 edn. Reterived form: http:// peer. berkeley. edu/ products /opensees.html.

USGS, 2012. US Geological Survey. Reterived form: http://www.usgs.gov/.

Vamvatsikos, D. and C.A. Cornell, 2002. Incremental dynamic analysis. Earthq Eng. Struct. Dyn., 31: 491-514.